5-2017

Accuracy of rainfall estimates at high altitude in the Garhwal Himalaya (India): A comparison of secondary precipitation products and station rainfall measurements

Alok BHARDWAJ

Alan D. ZIEGLER

Robert J. WASSON

Winston T. L. CHOW
Singapore Management University, winstonchow@smu.edu.sg

Atmospheric Research 188 (2017) 30–38

Contents lists available at ScienceDirect

Atmospheric Research

journal homepage: www.elsevier.com/locate/atmosres

Accuracy of rainfall estimates at high altitude in the Garhwal Himalaya (India): A comparison of secondary precipitation products and station rainfall measurements

Alok Bhardwaj [a,*], Alan D. Ziegler [a], Robert J. Wasson [b], Winston T.L. Chow [a]

[a] Department of Geography, National University of Singapore, Singapore
[b] Institute of Water Policy in the Lee Kuan Yew School of Public Policy, National University of Singapore, Singapore

ARTICLE INFO

Article history:
Received 23 August 2016
Received in revised form 28 December 2016
Accepted 10 January 2017
Available online 12 January 2017

Keywords:
Mandakini
Garhwal Himalaya
Secondary precipitation products

ABSTRACT

Accurate estimation of the magnitude and spatio-temporal variability of rainfall in the Indian Himalaya is difficult because of the sparse and limited network of ground stations located within complex terrain, as well as the difficulty of maintaining the stations over time. Thus, secondary rainfall sources are important to hydrological and hazard studies, if they reproduce the dynamics of rainfall satisfactorily. In this work, we evaluate four secondary products in the Garhwal Himalaya in India, with a focus on their application within the Mandakini River Catchment, the site of a devastating flood and multiple large landslides in 2013. The analysis included two satellite products: from the Tropical Rainfall Measuring Mission (TRMM) and the Precipitation Estimation from Remotely Sensed Information using Artificial Neural Networks (PERSIANN) program, as well as two gridded products: the Asian Precipitation Highly Resolved Observational Data Integration Towards Evaluation of Water Resources (APHRODITE) product and the India Meteorological Department (IMD) product. In comparing the four products against data collected at four ground stations (Rudraprayag, Joshimath, Purola, and Mukhim) using a variety of statistical indices, we determined that the IMD and TRMM products were superior to the others. In particular, the IMD product ranked the best for most indices including probability of detection (POD), false alarm ratio (FAR), receiver operating curve (ROC), and root mean squared error (RMSE). The TRMM product performed satisfactorily in terms of bias and detecting daily maximum monsoon rainfall at three of the four stations. The APHRODITE product had POD, FAR and ROC values that were among the best at higher rainfall depths at the Mukhim station. The PERSIANN product generally did not perform well based on these indices, consistently underestimating station rainfall depths. Finally, the IMD product could document the daily rainfall distribution during the June 2013 flood in the Mandakini Catchment and adjoining places.

1. Introduction

Precipitation is difficult to measure accurately in mountainous areas (Barros and Lettenmaier, 1994; Fang et al., 2013), particularly within very high and rugged mountains, such as in the Indian Himalaya (Barros et al., 2000; Bookhagen and Burbank, 2006; Burbank et al., 2012; Wulf et al., 2010). The need for measuring intense spatially-confined rainfall events in the Indian Himalaya is great because these events can generate (simultaneous) multiple hazards including large landslides, flash floods, landslide lake outburst floods (LLOFs), glacial lake outburst floods (GLOFs), and debris flows (Ziegler et al., 2014; Sati and Gahalaut, 2013; Kala, 2014). Landslides and LLOFs occur frequently in regions marked by faults, thrusts, and steep gradient streams in the Indian Himalaya (Wasson et al., 2013). High rainfall depths in general generate flash floods that further increase the frequency of other hazards by generating shallow landslides that contribute to debris flows and the formation of landslide lakes.

In a recent example in June 2013, Uttarakhand, a state in North India, witnessed a compound hazard consisting of a large flash flood, hundreds of shallow landslides, numerous LLOFs and a small GLOF in the Mandakini Catchment, which is located in the Upper Ganga Catchment (Kala, 2014; Sati and Gahalaut, 2013; Ziegler et al., 2014). The trigger of these cascading hazards was extreme rain falling over a 2-day period that totalled an estimated 300 mm of rainfall (Kala, 2014; Sati and Gahalaut, 2013; Dobhal et al., 2013).

Addressing the risk associated with extreme rainfall events in the Indian Himalaya requires understanding of the spatial distribution and intensity of rainfall. However, installing and maintaining a sufficient number of stations to record rainfall phenomena accurately is

* Corresponding author at: Department of Geography, AS2, #03-01, 1 Arts Link, Kent Ridge 117570, Singapore.
E-mail addresses: bhardwaj_alok@u.nus.edu (A. Bhardwaj), adz@nus.edu.sg (A.D. Ziegler), spprjw@nus.edu.sg (R.J. Wasson), winstonchow@nus.edu.sg (W.T.L. Chow).

http://dx.doi.org/10.1016/j.atmosres.2017.01.005
0169-8095/

complicated by rugged topography and inaccessibility of many locations, particularly those at higher elevations and on steep slopes. Thus, the region has a paucity of reliable recording stations, creating a sparse, non-uniform network of measurement points that generates limited data from which the spatio-temporal distribution of rainfall is difficult to determine accurately (Burbank et al., 2012).

Secondary sources of rainfall including satellite-based and gridded products with high spatial and temporal resolutions are potentially useful for examining the distribution of rainfall in mountains as they provide rainfall information at remote locations and are regularly updated to maintain complete data sets (Li et al., 2014). Satellite products are obtained through measurements of atmospheric properties by infrared (IR) and microwave sensors on-board satellites (Lo Conti et al., 2015). Gridded rainfall products are derived from station rainfall data that are first checked for quality and then mapped onto a spatial grid via interpolation (Pai et al., 2014; Yatagai et al., 2012). The temporal resolution of gridded products is typically coarse, for example daily or monthly. In comparison, satellite products may have sub-daily intervals.

We evaluate the accuracy of four secondary rainfall sources for estimating rainfall properties in the Garhwal Himalaya, with a special focus on the Mandakini Catchment. The secondary rainfall sources include the research-grade Tropical Rainfall Measuring Mission (TRMM) Multi-satellite Precipitation Analysis (TMPA) and the Precipitation Estimation from Remotely Sensed Information using Artificial Neural Networks (PERSIANN) products (Table 1). The two gridded products are the Asian Precipitation Highly Resolved Observational Data Integration Towards Evaluation of Water Resources (APHRODITE) and the India Meteorological Department (IMD) products (Table 1). The objective of our study is to determine the most appropriate product for studying rainfall-related hazards in the Garhwal Himalaya, including the 2013 Kedarnath Disaster in the Mandakini Catchment (Kala, 2014; Sati and Gahalaut, 2013; Ziegler et al., 2014).

2. Study area

The study area is the Mandakini Catchment and its vicinity in the neighbouring districts in the Garhwal Himalaya, located at the western end of the Central Himalaya (Fig. 1). The 2250 km^2 Mandakini Catchment stretches from Kedarnath in the north to Rudraprayag in the south, spanning latitudes 30o15'N to 30o45' N and longitudes 78o48'E to 79o20'E (Fig. 1). Elevations range from 700 to 3500 m in the Mandakini Catchment (Asthana and Sah, 2007). The Mandakini River joins the Alaknanda River at Rudraprayag.

The Mandakini River crosses the Main Central Thrust (MCT) that separates the Higher Himalaya from the Lesser Himalaya (Fig. 1). The MCT zone is composed of many faults, fractured and weathered rocks, high relief and, steep gradient streams with steep hill slopes along the stream edges (Asthana and Sah, 2007; Wasson et al., 2008). Steep slopes with loose material are susceptible to failures in response to various triggers, including earthquakes and high-intensity rainfall events during the monsoon season that accounts for 50–90% of total annual rainfall (Asthana and Sah, 2007; Larsen and Montgomery, 2012; Khandelwal et al., 2015).

Research on palaeo-floods in the upper Ganga Catchment within the Garhwal Himalaya (which includes the Mandakini, Bhagirathi and Alaknanda Catchments; Fig. 1) suggests that landslide lake outbursts flood during high-intensity monsoon rainfall are the primary cause of large floods (Wasson et al., 2013). For example, the June 2013 flash flooding in the Mandakini Catchment was likely exacerbated by LLOFs triggered by high-intensity rainfall over a 2-day period. The widespread damage in the catchment included thousands of deaths, destruction of infrastructure (e.g. roads, hydro-power), and loss of state tourism infrastructure and opportunities, as well as other livelihoods of local residents (Kala, 2014). The flood is now believed to be the largest in a millennium in this part of the Indian Himalaya (Wasson et al., 2013).

The flood destroyed the automatic weather station installed in the upper reaches of the Mandakini Catchment (Sati and Gahalaut, 2013), exacerbating the problem of limited data for assessment of hazards caused by rainfall in the Garhwal Himalaya.

Table 1
Name of secondary products of rainfall evaluated in this study with their spatial and temporal resolutions and availability.

Name	Spatial resolution	Temporal resolution	Availability
APHRODITE	0.25^0	Daily	1950–2007
IMD	0.25^0	Daily	1901–2013
PERSIANN	0.25^0	3-hourly	2000-present
TRMM	0.25^0	3-hourly	1998–2015

3. Methods

3.1. Station rainfall data

The four ground stations used in the study are located at (Table 2): (1) Rudraprayag in the Rudraprayag District; (2) Joshimath in the Chamoli District; (3) Purola in the Uttarkashi District; and (4) Mukhim in the Uttarkashi District (indicated by black circles in Fig. 1). Only the station at Rudraprayag is located within the Mandakini Catchment. The other three stations are located in the adjoining districts outside the catchment. Several other stations in the study area (indicated by white squares with black dot in Fig. 1) had incomplete data sets, and could not be used in the study. The four stations used in the study have rainfall data for most of the monsoon seasons from 2000 to 2007, which is the common period of rainfall data estimated by secondary products. The rainfall data for individual stations is administered by the India Meteorological Department (IMD); they are available at www.imdpune.gov.in. The rainfall data supplied by the IMD is quality checked to remove spurious data (Jaswal et al., 2014). In our study, we have checked all data to locate missing values and to properly account for them in the analysis.

3.2. Secondary products

The Asian Precipitation Highly Resolved Observational Data Integration Towards Evaluation of Water Resources (APHRODITE; Table 1) product is a high-resolution, daily, gridded precipitation dataset for the whole of Asia (Yatagai et al., 2012). The project assembles rainfall information from the Global Telecommunication System (GTS) network, precompiled datasets from meteorological organizations of Asian countries and APHRODITE's own rainfall datasets. For detailed information of each processing step used to build APHRODITE see Yatagai et al. (2012). Various APHRODITE products are available for several regions including Monsoon Asia (MA), Middle East (ME), Northern Eurasia (NE) and Japan. Our study utilizes the Monsoon Asia V1101 product obtained from the Research Institute for Humanity and Nature (RIHN) and the Meteorological Research Institute of Japan Meteorological Agency (MRI/JMA). The data are maintained at http://www.chikyu.ac.jp/precip/.

The Tropical Rainfall Measuring Mission (TRMM; Table 1) program was launched in 1997 as a joint effort by the National Aeronautics and Space Administration (NASA) and the Japan Aerospace Exploratory Agency (JAXA) to monitor tropical rainfall (Huffman et al., 2007). The passive microwave estimates of rainfall by TRMM Microwave Imager (TMI), together with passive microwave estimates from different low Earth orbit (LEO) satellites and infrared (IR) data collected by geosynchronous Earth orbit (GEO) satellites are collectively called as TRMM Multi-satellite Precipitation Analysis (TMPA) product. The TRMM Precipitation Radar (PR) data is used for calibrating the TMPA product. For details of the process to develop the TMPA product, see Huffman et al. (2007). The TRMM TMPA precipitation products are available in real time and research formats. The research product complements

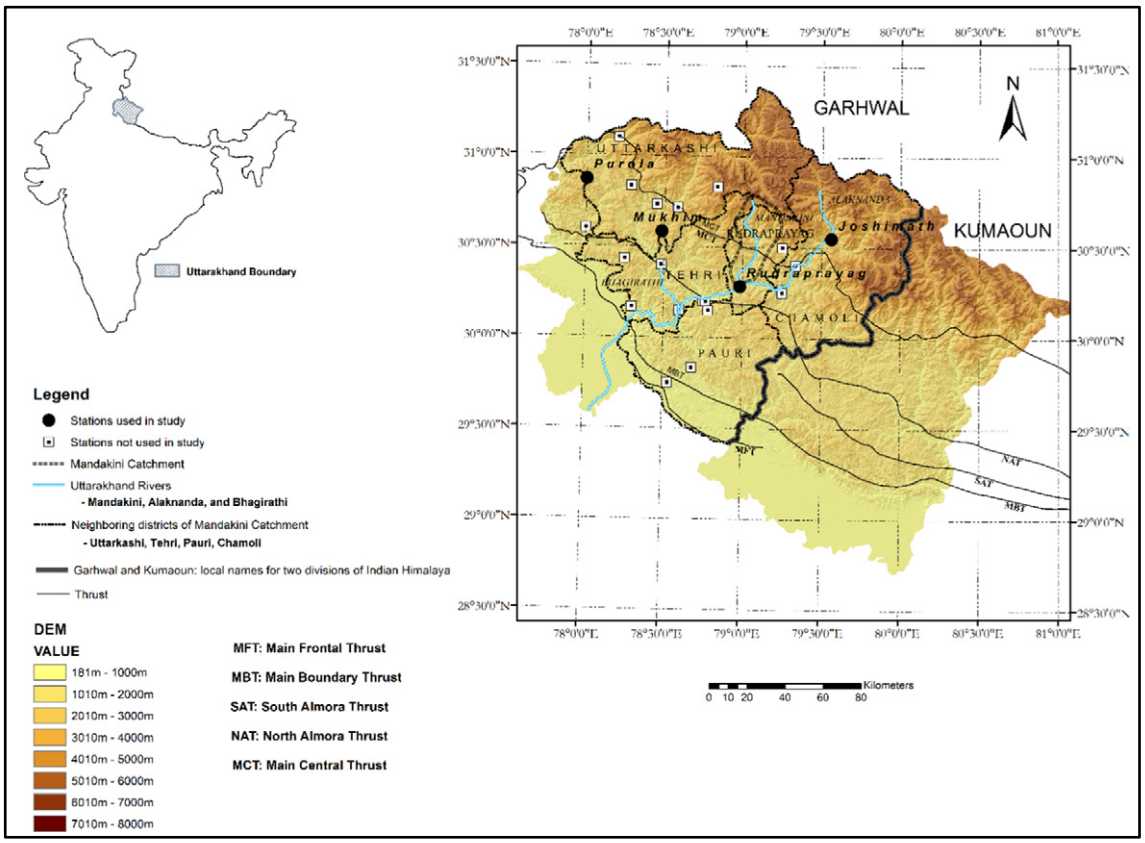

Fig. 1. Location of the four rainfall stations in the Garhwal Himalaya that are used in this study. Only one station at Rudraprayag is located in the Mandakini Catchment. The other three stations are located in adjoining districts. The rest of the stations located in the Garhwal Himalaya have many years of missing data and are not used in this study. The three main rivers of Uttarakhand are the Alaknanda, Mandakini and Bhagirathi Rivers.

the real-time product by including monthly ground estimates of rainfall from the Global Precipitation Climatology Project (GPCP). Our study utilizes the TMPA 3B42V7 research product that was retrieved from NASA's TRMM Online Visualization and Analysis System (TOVAS) at http://trmm.gsfc.nasa.gov/.

The Precipitation Estimation from Remotely Sensed Information using the Artificial Neural Networks (PERSIANN, Table 1) product is derived from IR data collected by geostationary satellites. The data are further updated by PMW rainfall estimates from low orbit microwave sensors using an adaptive artificial neural network (Hsu and Gao, 1997; Sorooshian et al., 2000). The bias within the PERSIANN product is adjusted by including total monthly precipitation information from the GPCP network of stations. (Lo Conti et al., 2015). Our study utilizes the bias adjusted PERSIANN product, which is available at the Center of Hydrometeorology and Remote Sensing (CHRS), University of California, Irvine at http://fire.eng.uci.edu/PERSIANN/adj_persiann_3hr.html.

The India Meteorological Department (IMD) developed a gridded daily rainfall dataset at 0.25° spatial resolution for the whole of India. A total of 6955 rainfall stations with varying periods of availability were used to compile the dataset. The raw data were first subjected to quality control to remove spurious data. The filtered data were interpolated onto a 0.25° gridded field using an inverse distance weighted interpolation scheme to create the final product. For more information on the methods used to develop the product see Pai et al. (2014). We obtained rainfall data from the IMD available at www.imdpune.gov.in.

The IMD and APHRODITE products are long-term data sets, while the TRMM and PERSIANN products have collected the majority of their rainfall data after 2000 (Table 1). Although the APHRODITE product ends in 2007, it is still useful to compare with other products because APHRODITE is a long-term data set with some data available for the Garhwal Himalaya. The common period for comparison of all products in this study is 2000 to 2007.

Table 2
Name of ground rainfall stations used in this study with their location, elevation and data availability.

Name	District	Elevation (m)	Availability
Rudraprayag	Rudraprayag	670	1996–2009
Joshimath	Chamoli	1875	1958–2008
Purola	Uttarkashi	1250	1980–2010
Mukhim	Uttarkashi	1981	1957–2007

3.3. Evaluation indices

We use continuous and categorical indices to evaluate the 'accuracy' of secondary rainfall products in reproducing rainfall depths at the four ground stations. The continuous indices mean bias error (MBE) and root mean square error (RMSE) were computed for daily rainfall depths of all monsoon seasons in all the years (2000–2007) with the following equations:

$$MBE = \frac{\sum_{i=1}^{n}(S_i - G_i)}{\sum_{i}^{n} G_i} \quad (1)$$

$$\mathrm{RMSE} = \sqrt{\frac{\sum_{i=1}^{n}(S_i - G_i)^2}{n}} \quad (2)$$

where S and G refer to rainfall depths estimated by secondary products and measured at ground stations, for the same days, respectively;

and 'n' refers to the total number of data points collected for all the 8 years during the monsoon season. In the MBE computation, rainfall days with zero rainfall are also included to avoid any asymmetry in the analysis. An MBE < 0 occurs when a secondary source underestimates station rainfall; alternatively, an overestimation occurs if MBE > 0 (Lo Conti et al., 2015, Li et al., 2014, Mantas et al., 2014).

Categorical indices include the probability of detection (POD) and the false alarm ratio (FAR). The POD is the fraction of the secondary source estimations that are in 'agreement' with measured station rainfall; agreement in this sense means that the depths of both measured and estimated rainfall exceed a given threshold (Lo Conti et al., 2015, Li et al., 2014, Mantas et al., 2014). The POD is determined as:

$$POD = \frac{r1}{(r1 + r3)} \quad (3)$$

where r1 is the number of data pairs of station and secondary product rainfall depths that exceed a certain threshold value and; r3 is the number of data pairs where station values are higher and secondary product values are smaller than the threshold (Table 3). In this analysis, the threshold in Table 3 refers to a depth of daily precipitation. The POD values range from 0 to 1: a POD value of 0 implies that the station and secondary product rainfall depths never simultaneously exceed a threshold value. A POD value of 1 is the best achievable score, which implies that the station measurements and secondary product estimates simultaneously exceeds a threshold at all times-thereby indicating similar behaviour.

The false alarm ration (FAR) is the fraction of detections by a secondary product that are incorrect or "false alarms" (Lo Conti et al., 2015, Li et al., 2014, Mantas et al., 2014).

$$FAR = \frac{r2}{(r1 + r2)} \quad (4)$$

where r1 and r2 are as in Table 3. In this analysis, a false alarm occurs when the estimates of rainfall by a secondary product exceed the threshold value but the measured rainfall depths at a station do not. The values of FAR range from 0 to 1. A FAR value of 0 is a perfect score, indicating no false alarm, which implies that a secondary product does not estimate rainfall higher than a threshold depth given a station records rainfall smaller than the threshold depth. A FAR value of 1 implies that rainfall depths detected by secondary products exceed a certain threshold but the station measurements of rainfall depths are lower than the threshold.

Table 3
Contingency table defining the criteria used in the calculation of POD (Eq. (3)), FAR (Eq. (4)), and FPR (Eq. (5)).

	Station rainfall > threshold*	Station rainfall ≤ threshold
Secondary Source rainfall > threshold	r1	r2
Secondary Source rainfall ≤ threshold	r3	r4

* r1 is the number of data pairs of both station and secondary product values that are greater than a certain threshold value; r2 is the number of data pairs where the station value is smaller than a threshold but the secondary product value is higher than the threshold; r3 is the inverse of r2; and r4 is the number of data pairs where both station and secondary product rainfall values are smaller than a certain threshold value. Threshold refers to a rainfall depth of daily precipitation. Threshold values used in this analysis are 0,1, 2, 3, 4, 5,10, 15,20, 25,30,35,40,45,50 mm. There are different r1, r2, r3 and r4 values for each threshold depth and for each secondary product at each station. For example, for IMD at Rudraprayag, r1, r2, r3 and r4 are 416, 227, 21 and 312 respectively for a threshold depth of 1 mm; 351, 200, 28 and 397 respectively for a threshold depth of 2 mm and so forth.

The false positive rate (FPR) indicates the percentage of rainfall events recorded by a secondary product that are not measured by a ground station.

$$FPR = \frac{r2}{(r2 + r4)} \quad (5)$$

where r2 and r4 are as in Table 3.

The receiver operating curve (ROC) is useful for summarizing the accuracy of secondary products, as it is used to identify secondary products that have higher POD and lower FPR values (Lo Conti et al., 2015).

As a final evaluation, we compare maximum daily rainfall detected by secondary products with depths measured by ground stations in the monsoon season of each year (i.e. one value per year). This comparison helps to understand the potential of secondary products to detect extreme rainfall events in the Garhwal Himalaya.

4. Results

4.1. Bias and error

The mean bias error calculations indicate that the PERSIANN product underestimates measured rainfall at all stations (MBE = −0.26 to −0.55; Table 4). This is observed in Fig. 2 (PERSIANN:1–4 plots), where most of the data pairs are below the 1:1 line, indicating under-estimation. The large negative MBE value of −0.55 indicates the substantial under-estimation that is observed in the PERSIANN-4 plot where few Mukhim rainfall values of up to 150 mm were detected only in the range of 0–20 mm in the PERSIANN product. The APHRODITE and TRMM products overestimated measured rainfall at three stations (Rudraprayag, Joshimath and Purola), but under-estimated it at Mukhim (Table 4). The high MBE value of 0.74 indicates large over-estimation by the APHRODITE product at Joshimath, which is also observed in the APHRODITE-2 plot where most of the data pairs are above the 1:1 line. At Mukhim, the APHRODITE-4 plot indicates under-estimation by the APHRODITE product (MBE = −0.26). A similar pattern in the MBE values is observed in TRMM:1–4 plots (Fig. 2) for the TRMM product.

The IMD product overestimates rainfall at Rudraprayag (MBE = 0.04) and Joshimath (0.56), but underestimates it at Purola (−0.17) and Mukhim (−0.25). These MBE values of the IMD product are reflected in the scatter plots IMD:1–4 of Fig. 2. The bias for the IMD product at Rudraprayag (0.04) was the lowest of all products, when all stations are considered (Table 4). At Purola and Mukhim the bias for IMD (−0.17 and −0.25, respectively) was not greatly different from those for TRMM (0.16 and −0.21) and APHRODITE (0.19 and −0.26). The main difference is the sign of the bias at Purola (i.e. IMD underestimates rainfall whereas the other two overestimate it). PERSIANN is the only product with reasonably low bias at Joshimath (−0.26); all other products over-estimate rainfall. Collectively, the MBE metric indicates IMD and TRMM have slightly less bias than the APHRODITE product. PERSIANN underestimates rainfall at all stations.

Table 4
Mean Bias Error (MBE; Eq. (1)) and Root Mean Square Error (RMSE; Eq. (2)) of each secondary product at each station. The values of MBE and RMSE are calculated for daily monsoon rainfall from 2000 to 2007.

		Rudraprayag	Joshimath	Purola	Mukhim
MBE	APHRODITE	0.14	0.74	0.19	-0.26
	IMD	0.04	0.56	-0.17	-0.25
	PERSIANN	-0.26	-0.26	-0.30	-0.55
	TRMM	0.25	0.73	0.16	-0.22
RMSE	APHRODITE	13.6	10.6	12.2	15.0
	IMD	**9.5**	**3.8**	**7.2**	**12.3**
	PERSIANN	14.5	9.4	12.2	23.3
	TRMM	14.5	11.1	10.7	20.2

Bold values represent the smallest RMSE values obtained for IMD at each station.

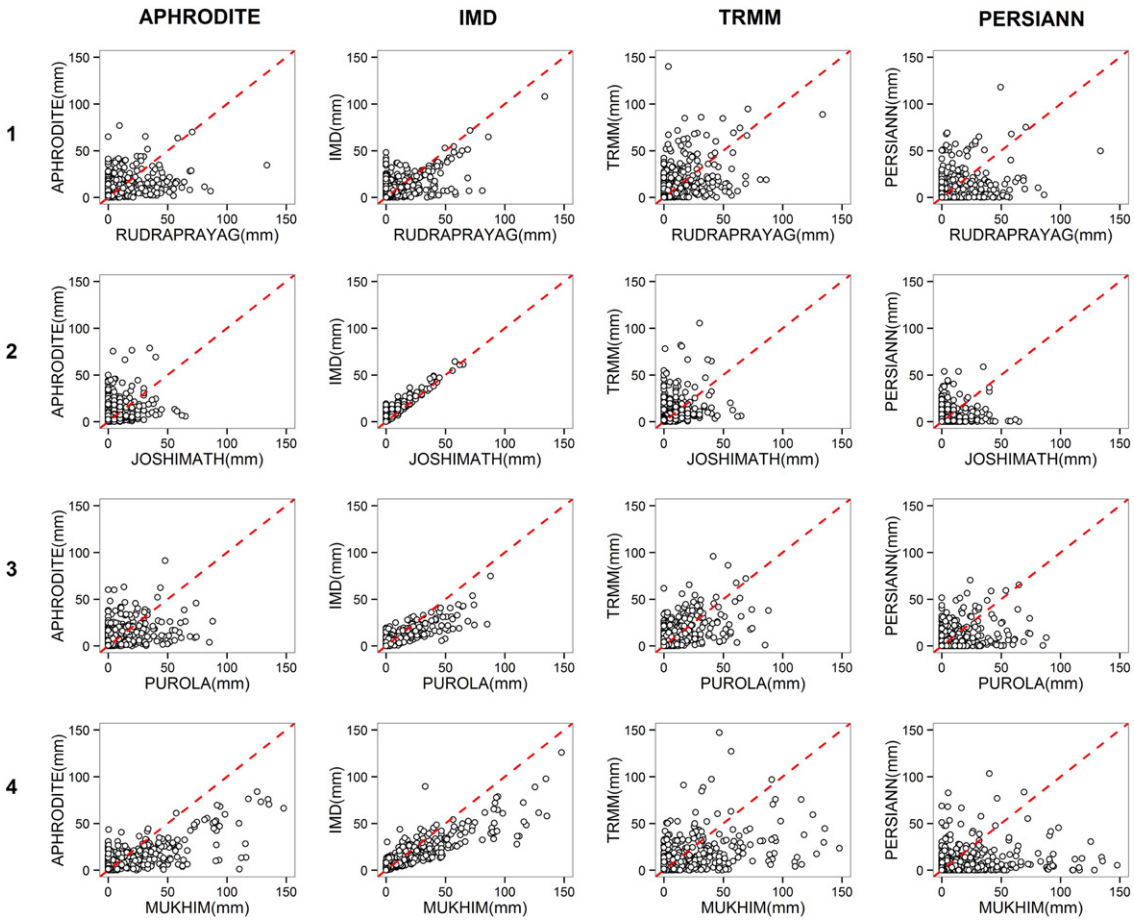

Fig. 2. Scatterplots of daily monsoon rainfall from 2000 to 2007 that is measured at each station and detected by each secondary product. Data pairs below the 1:1 line are under-estimated by secondary products and those above the line are over-estimated by secondary products.

The RMSE values are the lowest for the IMD product for all four stations (Table 4). Values range from 3.8 at Joshimath to 12.3 at Mukhim (Table 4). There is not a great difference in RMSE for APHRODITE, PERSIANN, and TRMM products at the four stations except at Mukhim where PERSIANN and TRMM have similarly high RMSE. The highest RMSE values for all products are at Mukhim; the lowest at Joshimath. Collectively, this index indicates that IMD is superior to the other products.

4.2. POD and FAR

The number of days a station records rainfall greater than a certain threshold (indicated by r1 + r3; Table 3) is shown in Fig. 3. Each station records fewer rainfall days as threshold magnitude is increased, implying that indices such as POD and FAR are calculated with fewer samples at higher thresholds than at smaller thresholds. The POD values for the IMD product are the highest at all stations other than Purola for rainfall

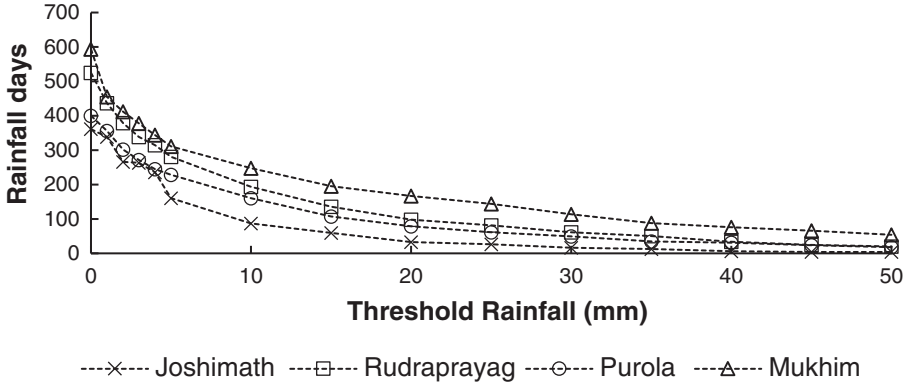

Fig. 3. Decrease in the number of rainfall days (r1 + r3; Table 3) as threshold magnitude is increased at each station. The number of rainfall days at each threshold for each station is calculated using the entire data set for all monsoon seasons from 2000 to 2007 after accounting for any missing values that are present in the dataset.

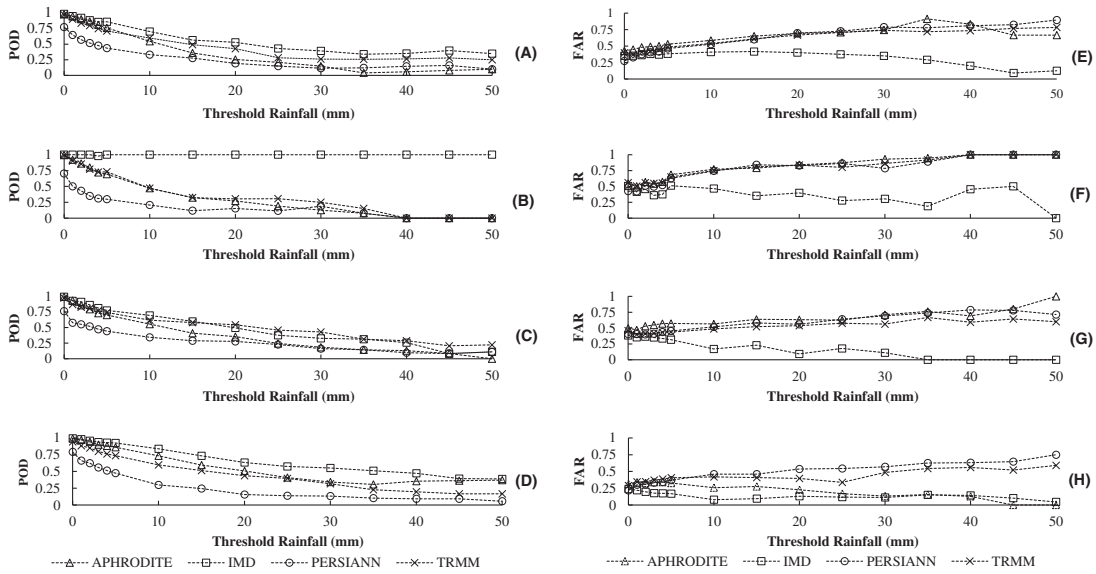

Fig. 4. Probability of Detection (POD; Eq. (3); A–D) and False Alarm Ratio (FAR; Eq. (4); E-H) for each secondary product at each station. Graphs (A, E) refers to Rudraprayag; (B, F) is Joshimath; (C, G) is Purola; and (D, H) is Mukhim. The POD is the fraction of secondary product estimations that agree with measured station rainfall (i.e. the depths of both estimated and measured rainfall exceed a given threshold). The FAR is the fraction of detections by a secondary source that are "false alarms". Threshold values used in this analysis are 0, 1, 2, 3, 4, 5, 10, 15, 20, 25, 30, 35, 40, 45 and, 50 mm.

depths >20 mm (Fig. 4 A-D). The PERSIANN product consistently has one of the lowest POD values at all stations and for all thresholds. The APHRODITE and TRMM products have POD values that are intermediate between those for the IMD and PERSIANN products. The TRMM product generally has similar or higher POD values than the APHRODITE product at all stations except at Mukhim (Fig. 4D). At Mukhim, the APHRODITE product had the best POD score, similar to the IMD product, for the two highest threshold depths. Collectively, by this index, the IMD product is superior to the others across all stations and for all thresholds.

The FAR values for the IMD product are consistently the lowest at all stations and for all thresholds (Fig. 4 E-H). The exception is at Mukhim, where the APRHODITE product has the lowest FAR values for thresholds in the range of 40–50 mm (Fig. 4H). The other three products have higher FAR values at all stations. Only at Mukhim, the TRMM and APHRODITE products have decreasing FAR values until the threshold depth of 25 mm, beyond which only the APRHODITE product has lower FAR values that are similar to or lower than those of the IMD product (Fig. 4H). Collectively, the FAR analysis shows that the IMD product is superior to the others.

Each data pair in the Receiver Operating Curve (ROC) plots corresponds to one threshold value (0, 1, 2, 3, 4, 5, 10, 15, 20, 25, 30, 35, 40, 45, 50 mm) (Fig. 5). Data pairs for all products plot above the 1:1 line, indicating each product detects rainfall accurately (values below the 1:1 line are considered inaccurate). By this metric, the best performing product is the IMD, which consistently has higher POD values and lower FPR values (Fig. 5). The APHRODITE and TRMM products both have higher FPR values, which indicate inaccurate estimations of measured rainfall. The PERSIANN product plots below all the other products as it has the lowest POD values, but also smaller FPR values. Collectively,

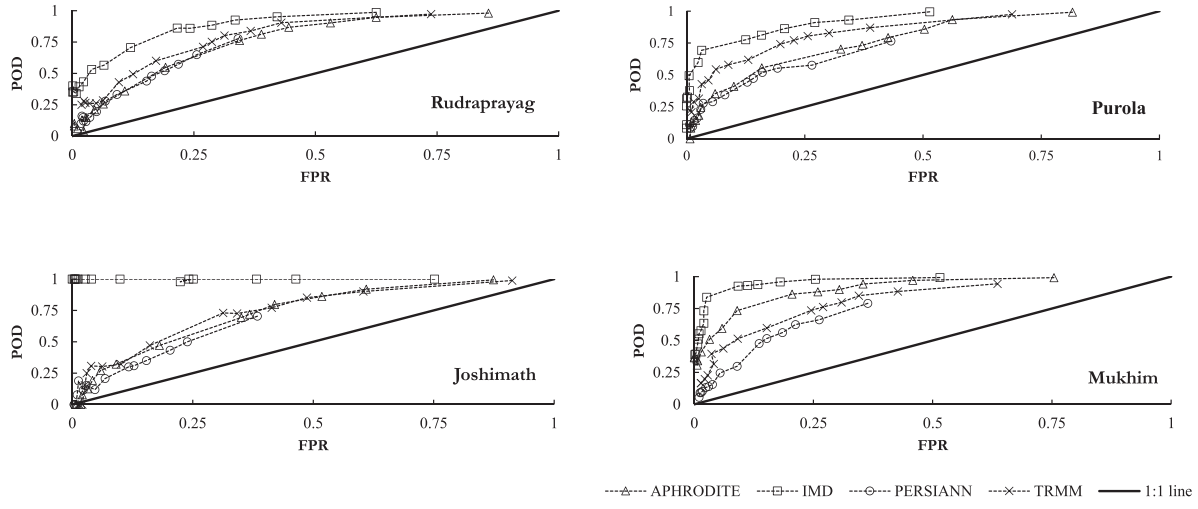

Fig. 5. Receiver Operating Curve (ROC) has Probability of Detection (POD; Eq. (3)) on the y-axis and the False Positive Rate (FPR; Eq. (5)) on the x-axis. The data pairs of POD and FPR are calculated for each secondary product at each of the four stations. The ROC is useful for summarizing the accuracy of secondary products, as it identifies the secondary products that have high POD and low FPR values.

Table 5
Mean Bias Error (MBE; Eq. (1)) values for comparing the daily maximum monsoon rainfall recorded by all secondary products at each station. Positive MBE values indicate over-prediction by secondary products while negative MBE values indicate under-prediction by secondary products.

		Rudraprayag	Joshimath	Purola	Mukhim
MBE	APHRODITE	−0.28	0.44	−0.27	−0.50
	IMD	−0.24	0.09	−0.38	−0.39
	PERSIANN	−0.16	0.09	−0.21	−0.45
	TRMM	0.08	0.67	−0.1	−0.30

the ROC curves indicate the superiority of IMD in reproducing measured rainfall with the least faulty detections.

4.3. Extreme rainfall

In the comparison of daily maximum monsoon rainfall estimated by secondary products and measured by ground stations, the MBE index (Eq. (1)) shows that the APHRODITE, IMD and PERSIANN products under-predict the daily maximum monsoon rainfall at all stations (except Joshimath) (Table 5). The highest under-prediction (negative MBE values) were at Mukhim, as seen in the plot for which secondary product rainfall depths are smaller than Mukhim rainfall (Fig. 6). All four products over-predict the daily maximum monsoon rainfall at Joshimath as indicated by the positive values of MBE (Table 5). The TRMM product shows the highest over-prediction (0.67) at this station, which is also observed in Fig. 6. The TRMM product also over-predicts at Rudraprayag (0.08), but under-predicts at Purola (−0.1) and Mukhim (−0.3). Collectively, the smallest values of MBE (not considering the sign of MBE) are obtained for TRMM at three stations (except Joshimath) and, for IMD and PERSIANN at Joshimath. By this metric, the TRMM product is the best for predicting daily maximum monsoon rainfall in the Garhwal Himalaya.

5. Discussion

5.1. The most accurate secondary product

When all the metrics used to examine the accuracy of the four secondary products are considered (Table 6), the IMD product emerges as the most accurate for the Mandakini study site. Firstly, the IMD product shows the least bias (MBE), except at Joshimath, and it has the lowest RMSE at all stations. As indicated by the POD and FAR indices, the IMD product was the top-ranking product at two stations, and was one of the top two products at Purola and Mukhim for a short range of threshold depths. The receiver operating curves were also the most favourable for the IMD product at all stations, indicating that this product is the best at predicting threshold rainfall depths at all stations. However, the IMD product was inferior to the TRMM product in detecting daily maximum monsoon rainfall at three stations but not at Joshimath. Collectively, the metrics with the exception of extreme rainfall, support IMD as the most accurate secondary product. The inaccurate estimates of TRMM and PERSIANN could be attributed to many factors such as errors due to retrieval algorithm, instrument, georeferencing, spatial sampling, topography, and relief (Andermann et al., 2011, Krajewski, 2007). The calibration of IR sensor observations of cloud-top temperature may also introduce uncertainty in estimates of precipitation (Huffman et al., 2007). The lower performance of APHRODITE could be explained by the non-availability of many stations on a given day for interpolation of rainfall (Yatagai et al., 2012).

Table 6
Table values indicate the product that performed the 'best' based on the identified metric. More than one entry implies two or more products were similar in performance, with the ordering indicating performance. A refers to APHRODITE; I, IMD; P, PERSIANN; and T, TRMM. MBE is mean bias error (Eq. (1)); RMSE, root mean square error (Eq. (2)); POD, Probability of detection (Eq. (3)); FAR, false alarm ratio (Eq. (4)); ROC, receiver operating curves (Section 4.2); and extreme RF, maximum daily rainfall value in monsoon season each year (Section 4.3).

	Rudraprayag	Joshimath	Purola	Mukhim
MBE	I	P	T, I, A	T, I, A
RMSE	I	I	I	I
POD	I	I	I, T	I, A
FAR	I	I	I	I, A
ROC	I	I	I	I
Extreme RF	T	I ~ P	T	T

5.2. Uttarakhand flood

A devastating flood happened in the Mandakini Catchment in early June 2013 following a high intensity rainfall event (Kala, 2014; Ziegler et al., 2014). The flood devastated a major portion of this catchment and other areas in Uttarakhand. It is important to test the application of secondary products to predict rainfall during the flood because ground stations may not properly function during storms. For example, the automatic weather station near Chaurabari Glacier was destroyed by the flood (Sati and Gahalaut, 2013). We have evaluated secondary

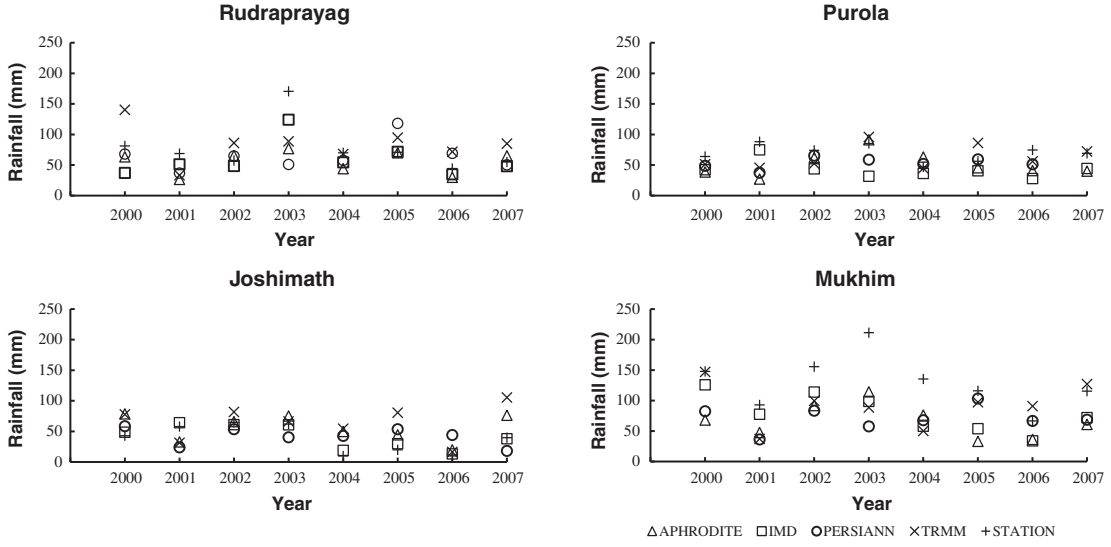

Fig. 6. Comparison of daily maximum monsoon rainfall detected by secondary products to daily maximum monsoon rainfall measured by stations in years 2000–2007. For each rainfall source one value of daily maximum rainfall in the monsoon season of each year is plotted and compared with those of others.

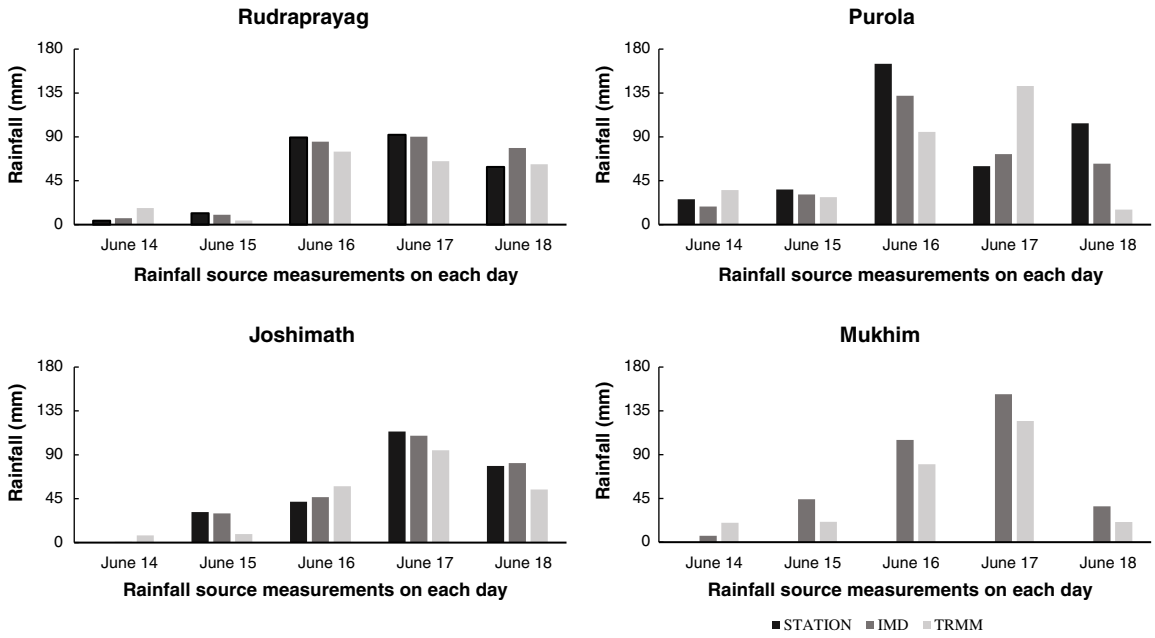

Fig. 7. Comparison of daily rainfall depth measured at all stations (except Mukhim) with the predictions of the IMD and TRMM products from June 14 to June 18, 2013 in the Garhwal Himalaya. A large flash flood occurred in the Mandakini Catchment during these dates.

products, IMD and TRMM, for predicting rainfall at Rudraprayag, Joshimath, and Purola. Unfortunately, ground station data for Mukhim were not available for this period and PERSIANN product will be available in future. In this analysis, we compared secondary products to ground station data from June 14 to June 18 (IMD, 2013) (Fig. 7). The ground station data at three stations were collected using standard rain gauges (IMD, 2014) that may not function properly during high intensity rainfall events. However, the gauge data are quality checked to remove spurious values (Jaswal et al., 2014). This again shows the increasing need to use secondary products to estimate rainfall in the Indian Himalaya and particularly in the Mandakini Catchment.

The IMD product performed better than the TRMM product in predicting ground station rainfall on June 16 and 17, two days when the highest rainfall was measured. The IMD product predictions were similar at all stations except at Purola on June 16. The TRMM product either under-predicted or over-predicted station rainfall on both days. On June 18, the TRMM product had improved performance at Rudraprayag and the IMD product at Joshimath. At Purola, both products underestimated station rainfall. On June 14 and 15, records of smaller rainfall depths were reflected in the predictions of the IMD and TRMM products. On both days, the IMD product estimation was more accurate than that of the TRMM product. The Mukhim rainfall data were not available, nonetheless IMD and TRMM estimates are used for comparison. The TRMM product estimated smaller rainfall depths than the IMD product. Considering all the days, the IMD product was better than the TRMM product at estimating daily rainfalls during the 2013 flood in the Garhwal Himalaya.

6. Conclusion

The purpose of our study was to evaluate secondary rainfall products that could be used to estimate rainfall in the Indian Himalaya with a focus on the Mandakini Catchment, which was the site of a devastating flood in June 2013. As ground station data are limited in this area of the world, secondary satellite and/or gridded products are potentially useful for hydrological and hazard studies. We found the TRMM and PERSIANN satellite products and the gridded APHRODITE and IMD products have high spatial and temporal coverage that record the rainfall distribution in the mountain with varying degrees of accuracy. The performance of IMD was higher than other products when compared with data from four ground stations. The TRMM product also performed satisfactorily for a few indices. The IMD was the best overall product, and TRMM was the highest performing satellite product. Important for hazard studies, we believe the IMD product with 113 years of rainfall data is useful for studying long-term trends of rainfall, including extreme events in the Indian Himalaya. Improved calibrations of microwave and infra-red sensors are still needed in the Indian Himalaya.

Acknowledgement

This work was supported by the NUS Research Scholarship and two research grants namely R-109-000-134-112 and R-109-000-174-646 held by the Department of Geography, NUS. We also thank Department of Earthquake Engineering, IIT Roorkee, India for providing the IMD data set. We thank IMD for providing their gridded rainfall dataset and rainfall data for individual stations. We also thank NASA for making TRMM data sets freely available to the scientific community. We acknowledge the efforts of the Center of Hydrometeorology and Remote Sensing (CHRS), University of California, Irvine, for maintaining and updating PERSIANN. We also appreciate the effort of the Research Institute for Humanity and Nature (RIHN) and the Meteorological Research Institute of Japan Meteorological Agency (MRI/JMA) for maintaining and updating APHRODITE and making it freely available to the scientific community.

References

Andermann, C., Bonnet, S., Gloaguen, R., 2011. Evaluation of precipitation data sets along the Himalayan front. Geochem. Geophys. Geosyst. 12 (7).
Asthana, A.K.L., Sah, M.P., 2007. Landslides and cloudbursts in the Mandakini Basin of Garhwal Himalaya. Himal. Geol. 28 (2), 59–67.
Barros, A.P., Lettenmaier, P., 1994. Dynamic modeling of orographically induced precipitation. Rev. Geophys. 32 (3), 265–284.
Barros, A.P., Joshi, M., Putkonen, J., Burbank, D.W., 2000. A study of 1999 monsoon rainfall in a mountainous region in central Nepal using TRMM products and rain gauge observations. Geophys. Res. Lett. 27 (22), 3683–3686.
Bookhagen, B., Burbank, D.W., 2006. Topography, relief, and TRMM-derived rainfall variations along the Himalaya. Geophys. Res. Lett. 33 (8), L08405.
Burbank, D.W., Bookhagen, B., Gabet, E.J., Putkonen, J., 2012. Modern climate and erosion in the Himalaya. Compt. Rendus Geosci. 344 (11–12), 610–626.

Dobhal, D.P., Gupta, A.K., Mehta, M., Khandelwal, D.D., 2013. Kedarnath disaster: facts and plausible causes. Curr. Sci. 105 (2), 171–174.
Fang, J., Du, J., Xu, W., Peijun, S., Li, M., Ming, X., 2013. Spatial downscaling of TRMM precipitation data based on the orographical effect and meteorological conditions in a mountainous area. Adv. Water Resour. 61, 42–50.
Hsu, K., Gao, X., 1997. Precipitation estimation from remotely sensed information using artificial neural networks. J. Appl. Meteorol. 36, 1176–1190.
Huffman, G.J., Adler, R.F., Bolvin, D.T., Gu, G., Nelkin, E.J., Bowman, K.P., Hong, Y., Stocker, E.F., Wolff, D.B., 2007. The TRMM Multisatellite Precipitation Analysis (TMPA): quasi-global, multiyear, combined-sensor precipitation estimates at fine scales. J. Hydrometeorol. 8 (1), 38–55.
IMD, 2013. A preliminary report on heavy rainfall over Uttarakhand during 16–18 June 2013. India Meteorological Department, Ministry of Earth Sciences (Accessed on 04/09/2013. http://imd.gov.in/doc/uttarakhand_report_04_09_2013.pdf).
IMD, 2014. Monsoon 2013. A report on various aspects of operational monitoring and forecasting of observed weather and climate features of 2013 SW monsoon. Accessed on 10/10/2014. http://www.imdpune.gov.in/monsoon_report_2013.pdf.
Jaswal, A.K., Narkhede, N.M., Shaji, R., 2014. Atmospheric data collection, processing and database management in India Meteorological Department. Proc. Indian Natl. Sci. Acad. 80 (3), 697–704.
Kala, C.P., 2014. Deluge, disaster and development in Uttarakhand Himalayan region of India: challenges and lessons for disaster management. Int. J. Disaster Risk Reduct. 8, 143–152.
Khandelwal, D.D., Gupta, A.K., Chauhan, V., 2015. Observations of rainfall in Garhwal Himalaya, India during 2008–2013 and its correlation with TRMM data. 108 (6), 1146–1151.
Krajewski, W., 2007. Ground networks. Are we doing the right thing? In measuring precipitation from space – EURAINSAT and the future. pp. 403–417 (ISBN: 13978-1-4020-5835-6).
Larsen, I.J., Montgomery, D.R., 2012. Landslide erosion coupled to tectonics and river incision. Nat. Geosci. 5 (7), 468–473.
Li, X., Zhang, Q., Xu, C.Y., 2014. Assessing the performance of satellite-based precipitation products and its dependence on topography over Poyang Lake basin. Theor. Appl. Climatol. 115 (3–4), 713–729.
Lo Conti, F., Hsu, K.-L., Noto, L.V., Sorooshian, S., 2015. Evaluation and comparison of satellite precipitation estimates with reference to a local area in the Mediterranean Sea. Atmos. Res. 138, 189–204.
Mantas, V.M., Liu, Z., Caro, C., Pereira, A.J.S.C., 2014. Validation of TRMM multi-satellite precipitation analysis (TMPA) products in the Peruvian Andes. Atmos. Res. 163, 132–145.
Pai, D.S., Sridhar, L., Rajeevan, M., Sreejith, O.P., Satbhai, N.S., Mukhopadyay, B., 2014. Development of a new high spatial resolution ($0.25^\circ \times 0.25^\circ$) long period (1901–2010) daily gridded rainfall data set over India and its comparison with existing data sets over the region. Mausam 65 (1), 1–18.
Sati, P., Gahalaut, V.K., 2013. The fury of the floods in the north-west Himalayan region: the Kedarnath tragedy. Geomat. Nat. Haz. Risk 4 (3), 193–201.
Sorooshian, S., Hsu, K.L., Gao, X., Gupta, H.V., Imam, B., Braithwaite, D., 2000. Evaluation of PERSIANN system satellite-based estimates of tropical rainfall. Bull. Am. Meteorol. Soc. 81 (9), 2035–2046.
Wasson, R.J., Juyal, N., Jaiswal, M., McCulloch, M., Sarin, M.M., Jain, V., Srivastava, P., Singhvi, A.K., 2008. The mountain-lowland debate: deforestation and sediment transport in the upper Ganga catchment. J. Environ. Manag. 88 (1), 53–61.
Wasson, R.J., Sundriyal, Y.P., Chaudhary, S., Jaiswal, M.K., Morthekai, P., Sati, S.P., Juyal, N., 2013. A 1000-year history of large fl oods in the Upper Ganga catchment, central Himalaya, India. Quat. Sci. Rev. 77, 156–166.
Wulf, H., Bookhagen, B., Scherler, D., 2010. Seasonal precipitation gradients and their impact on fluvial sediment flux in the Northwest Himalaya. Geomorphology 118 (1–2), 13–21.
Yatagai, A., Kamiguchi, K., Arakawa, O., Hamada, A., Yasutomi, N., Kitoh, A., 2012. APHRODITE: constructing a long-term daily gridded precipitation dataset for Asia based on a dense network of rain gauges. Bull. Am. Meteorol. Soc. 93 (9), 1401–1415.
Ziegler, A.D., Wasson, R.J., Bhardwaj, A., Sundriyal, Y.P., Sati, S.P., Juyal, N., Nautiyal, V., Srivastava, P., Gillen, J., Saklani, U., 2014. Pilgrims, progress, and the political economy of disaster preparedness - the example of the 2013 Uttarakhand flood and Kedarnath disaster. Hydrol. Process. 28 (24), 5985–5990.